agronomy

Article

Response of Water Radiation Utilization of Summer Maize to Planting Density and Genotypes in the North China Plain

Zhendong Liu, Shiyu Wei, Ming Li, Qingfen Zhang, Rui Zong and Quanqi Li *

College of Water Conservancy and Civil Engineering, Shandong Agricultural University, Tai'an 271018, China
* Correspondence: quanqili@sdau.edu.cn

Abstract: Increasing the planting density of summer maize to improve the utilization efficiency of limited soil and water resources is an effective approach; however, how the leaf water-use efficiency (WUE_L), yield, and RUE respond to planting density and genotypes remains unclear. A 2-year field experiment was performed in the North China Plain (NCP) to investigate the effects of planting density (high, 100,000 plants ha^{-1}; medium, 78,000 plants ha^{-1}; and low, 56,000 plants ha^{-1}) and genotypes (Zhengdan 958 and Denghai 605) on the leaf area index (LAI), photosynthetic characteristics, dry-matter accumulation, WUE_L, and RUE of maize. The objective was to explore the effect of density and genotype on the WUE_L and RUE of maize. Increasing planting density boosted LAI, light interception, dry-matter accumulation, and spike number but reduced the chlorophyll content, net photosynthetic rate, transpiration rate, and 1000-kernel weight. Both high and low planting densities were averse to RUE and yield. Zhengdan 958 increased the WUE_L by 19.45% compared with Denghai 605, but the RUE of Denghai 605 was 18.19% higher than Zhengdan 958, suggesting that Denghai 605 had a greater production potential as the planting density increased. Our findings recommend using 78,000 plants ha^{-1} as the planting density with Denghai 605 to maintain summer maize yields in the NCP.

Keywords: chlorophyll content index; leaf area index; leaf water-use efficiency; radiation-use efficiency; yield

Citation: Liu, Z.; Wei, S.; Li, M.; Zhang, Q.; Zong, R.; Li, Q. Response of Water Radiation Utilization of Summer Maize to Planting Density and Genotypes in the North China Plain. *Agronomy* **2023**, *13*, 68. https://doi.org/10.3390/agronomy13010068

Academic Editor: J. Stephen C. Smith

Received: 26 November 2022
Revised: 21 December 2022
Accepted: 22 December 2022
Published: 25 December 2022

1. Introduction

Food security has become a growing global challenge for the world [1]. According to data released by the World Food and Agriculture Organization of the United Nations (2022), the number of hungry people worldwide was 828 million in 2021, and the global population affected by food shortages will not decrease in the following decade (www.fao.org [accessed on 1 October 2022]). The imbalance between food demand and agricultural resources is the most prominent challenge in global resource protection and rational utilization, and it is becoming increasingly serious with population growth. Improving land productivity and agricultural resource utilization efficiency is necessary to mitigate this challenge [2]. Wheat, maize, and rice are the main food crops worldwide, and the planting area of each crop exceeds 200 million hectares. Among them, maize, which is distributed over a wider area, has better environmental adaptability [3]. China is the main maize producer, and according to statistics from the State Statistical Bureau (China), the maize planting area in 2021 in China reached 430 million hectares (www.stats.gov.cn [accessed on 1 October 2022]). China's important maize production base is the North China Plain (NCP) [4]. China has only 9% of the world's arable land and 6% of the world's total water resources; however, it provides food for 22% of the world's population [5]. Limited freshwater resources greatly challenge agricultural sustainability and development; therefore, the development of high-water-use efficient agriculture is urgent [6].

To balance the huge demand for grain production and limited land resources, increasing planting density is generally considered a key solution to improve land productivity and crop yield [7]. However, high plant density reduces the light intensity reaching the lower canopy, consequently reducing the crop function of the lower canopy, resulting in low utilization of nutrients and light resources by plants, adversely affecting crop yield [8,9]. In addition, maize is sensitive to soil moisture [10]. Improper planting patterns generally accelerate water and land resource shortages [11,12], threatening regional food supplies [13]. Plant density is also a crucial factor influencing crop biomass formation [14].

Photosynthesis is a crucial metabolic process in plants that determines the transport and partitioning of photoassimilates [15]. The photosynthetic intensity is generally controlled by chloroplast structure and chlorophyll concentration [16]. Through chlorophyll, green plants transform light energy into chemical energy, and chlorophyll concentration is usually adopted to evaluate the photosynthetic dynamics of leaves [17]. For example, Huang et al. [18] found that higher chlorophyll content improved the photosynthetic performance of leaves. Enhanced photosynthesis was beneficial in improving the radiation-use efficiency (RUE) and water-use efficiency of leaves (WUE_L), increasing leaf transpiration rate, boosting the nutrient utilization rate of plants [19], and improving water-use efficiency [20]. In addition, the filling stage is a key period for grain formation in summer maize [21]. The dry matter of grains is influenced by the filling rate and time, which largely depend on genotype and environmental factors [22], such as drought stress, planting density, and light intensity [23].

One of the most significant environmental factors that affect plant growth and grain development is light intensity [24]. As a C4 plant, maize is highly sensitive to light intensity, and its growth requires rich sunlight resources [25]. Photosynthetically active radiation (PAR) is closely related to the energy transformation and material production processes of plants and is the primary energy source for biomass formation [26,27]. Specifically, green plants use PAR from sunlight and CO_2 in the atmosphere to generate chemical energy through photosynthesis, thus providing nutrition for almost all living organisms on Earth [28]. Therefore, the interception of solar radiation is vital for the growth of summer maize under field conditions [29]. In summer maize, the absorption of solar radiation is also affected by the leaf area index (LAI) [30,31]. The leaves convert the intercepted solar radiation into dry matter above ground [32]. The accumulation of dry matter above the ground further affects the summer maize yield [33]. Crop productivity in dryland agriculture is strongly correlated with the efficiency of converting water and solar radiation into dry-matter accumulation [34].

Canopy structure is an important feature of agricultural ecosystems that affects water–carbon cycling, the microclimate, and crop competitiveness [35–38]. Changes in plant density can cause significant changes in the canopy structure and further affect the interception of light radiation [39–41]. An appropriate planting density can adjust the canopy structure of summer maize and improve the light distribution in the canopy for improving the efficiency of light energy utilization [42]. For example, Shi et al. [43] showed that increasing density improves LAI when the density is 82,500 plants ha^{-1}, with the summer maize having the highest RUE. Chen et al. [44] reported that when the density of maize increased from six to nine plants m^{-2}, the water-use efficiency also increased. However, if LAI increases too high, it may result in self-shading and even yield loss [45]. The ideal LAI has been shown in earlier investigations to be higher than 10 [46]. However, according to Kiniry et al. [47], the ideal LAI for maize was 6. Therefore, choosing the right planting density will enhancing the yield and RUE.

Previous studies have only reported a single effect of planting density or genotype on maize growth. For example, Shi et al. [48] showed that increasing the planting density of maize significantly improved the biomass and LAI of maize after flowering, and the distribution and absorption of light in the maize canopy under high-density treatment were different from those under low-density treatment. Liu et al. [49] revealed that different genotypes showed different canopy interception ratios, accumulation levels of dry matter, and yield. However, the changes in the WUE_L, RUE, and yield of summer maize under the combination of planting density and genotype remain unclear. Therefore, in our research, we selected two key factors related to limiting the use of solar radiation and water resources, i.e., density and genotype. We hypothesized that more drought-resistant genotypes of maize combined with appropriate planting density could greatly increase solar radiation and water utilization efficiency, mitigating the shortage of cultivated land and freshwater resources. In this study, two summer maize genotypes with various levels of drought resistance in NCP and three planting densities were selected. We determined the effects of planting density and summer maize genotype on canopy structure, PAR, WUE_L, yield, and RUE. In this study, our goal is to investigate the following: (1) study the effect of density and genotype on WUE_L and RUE of summer maize; (2) determine the yield of summer maize with different planting densities and genotypes. Our findings can provide theoretical value for maintaining summer maize yields in the NCP.

2. Materials and Methods

2.1. Experimental Station

The experiment was carried out during the summer maize growing seasons in 2021 and 2022 under rain-fed conditions at the Agronomy Experiment Station of Shandong Agricultural University (36°10′9″ N, 117°9′03″ E). The experimental station is in the temperate continental monsoon climate zone, with an average annual rainfall from June to September of 453.7 mm. The soil of the experimental site is loamy (40% sand, 44% silt, and 16% clay), with total nitrogen, available phosphorus, and available potassium contents of 108.3 m kg^{-1}, 16.2 mg kg^{-1}, and 92.6 mg kg^{-1} in the 0–20 cm soil layer, respectively. In the 2021 and 2022 summer maize growing seasons, the precipitation was 691 mm and 532 mm, respectively. The precipitation and temperature during June to September of the test are shown in Figure 1. An on-site weather station (NL–GPRS–1, Zhejiang Top Cloud-agri Technology Co., Ltd., Zhejiang, China) was used to recorded the weather information (precipitation, minimum and maximum temperatures, and solar radiation) near the study site.

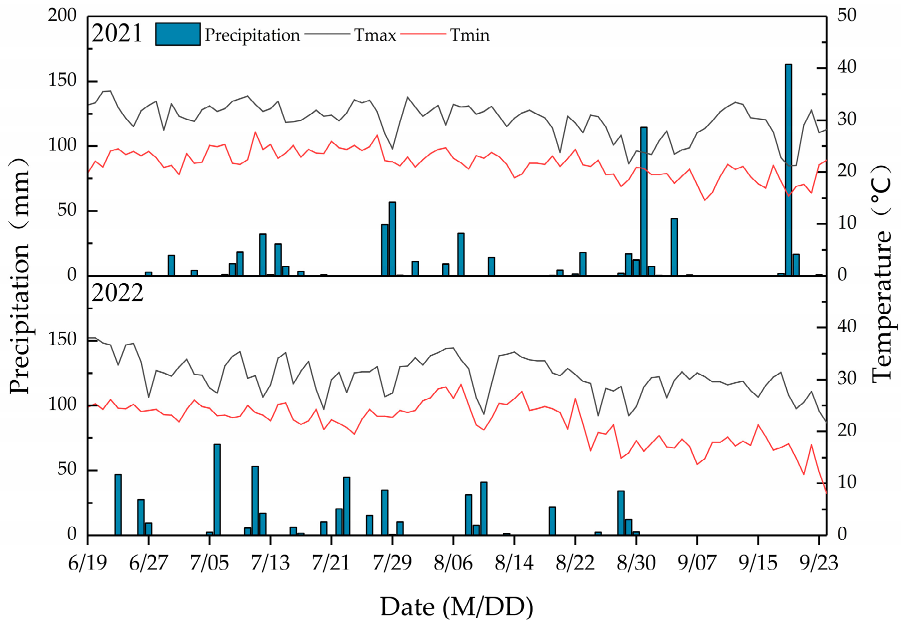

Figure 1. Daily maximum temperature (Tmax), daily minimum temperature (Tmin), and daily precipitation at the experimental station during the 2021 and 2022 summer maize growing seasons.

Summer maize was planted in experimental plots with an area of 3 m × 3 m, surrounded by bricks and concrete (1.50 m deep) to prevent the horizontal flow of water.

2.2. Experimental Design

A split-plot design with a random zone arrangement was used for the experiment. Three planting patterns, including high (H, 100,000 plants ha^{-1}), medium (M, 78,000 plants ha^{-1}), and low (L, 56,000 plants ha^{-1}) densities, were the main divisions, and two genotypes, Zhengdan 958 (Z) and Denghai 605 (D), were the subdivisions. Z (Henan Academy of Agricultural Sciences Institute of Grain Crops; Zhengzhou, Henan, China) was the drought-resistant. D (Shandong Denghai Seed Industry Co., Ltd.; Laizhou, Shandong, China) was the drought-sensitive. There were six treatments in total, and each treatment was repeated thrice. A total of 18 plots were randomly arranged into blocks. The row spacing of summer maize was 60 cm. Summer maize was planted on 20 June 2021 and 19 June 2022, then harvested on 24 September 2021 and 24 September 2022. In the two years, the accumulated rainfall in the week before sowing was 75.5 mm and 22.2 mm, respectively, so we irrigated before sowing at 60 mm in 2022. The irrigation method was flood irrigation. Before sowing, 22.50 g m^{-2} of urea, 16.90 g m^{-2} potassium chloride, and 22.50 g m^{-2} diammonium phosphate were applied as base fertilizers in each plot. Topdressing urea was applied at the V6 (the sixth-leaf stage) with 22.50 g m^{-2}. Other field management practices referred to local experiences.

2.3. Measurements

2.3.1. Leaf Area Index

At V6, V12 (the twelfth-leaf stage), R1 (silking stage), and R2 (filling stage) of summer maize, we selected three uniform-growth plants from each plot and measured the length and maximum width of all leaves. LAI was calculated as follows [50]:

$$\text{Leaf area per plant} = \sum_{i=1}^{n} \mathrm{k}(\mathrm{L_i} \times \mathrm{B_i}) \tag{1}$$

$$\text{Leaf area index (LAI)} = \text{leaf area per plant} \times \text{number of plants per unit area} \tag{2}$$

where k is the leaf area conversion coefficient, the fully developed leaf k is 0.75, the undeveloped leaf k is 0.50, L is the leaf length, B is the maximum leaf width, and subscript i is the number of leaves.

2.3.2. Photosynthetically Active Radiation

During R2 of summer maize, PAR measurements were conducted from 9:00 to 11:00 on typical sunny days. The test data were collected through a linear sensor using the SunScan canopy analyzer (Delta-T Devices Ltd., Cambridge, UK) The sensor was placed parallel between two adjacent rows of summer maize and parallel to the ground. The incident and reflected PAR were measured at the top, middle, and bottom of the canopy of the summer maize. The bottom data were measured at 10 cm higher than ground. PAR interception, penetration, and reflection ratio of the entire canopy were calculated as follows [16]:

$$\text{Canopy PAR interception ratio} = \frac{\left[\mathrm{in_{(c)}} - \mathrm{re_{(c)}} - \mathrm{in_{(g)}} + \mathrm{re_{(g)}}\right]}{\mathrm{in_{(c)}}} \times 100\% \tag{3}$$

$$\text{Canopy PAR penetration ratio} = \frac{\mathrm{in_{(g)}}}{\mathrm{in_{(c)}}} \times 100\% \tag{4}$$

$$\begin{gathered}\text{Canopy reflection ratio of canopy } = \\ (1 - \text{Canopy PAR interception ratio } - \text{Canopy PAR penetration ratio}) \times 100\%\end{gathered} \tag{5}$$

where $\mathrm{in_{(c)}}$ is the incidence of the canopy, $\mathrm{in_{(g)}}$ is the incidence of the stratum, $\mathrm{re_{(c)}}$ is the reflection of the canopy, and $\mathrm{re_{(g)}}$ is the reflection of the bottom.

The PAR interception ratio in the middle of the canopy was calculated as follows:

$$\text{The PAR interception ratio at the middle of canopy} = \frac{\left[\text{in}_{(s)} - \text{re}_{(s)} - \text{in}_{(g)} + \text{re}_{(g)}\right]}{\text{in}_{(c)}} \times 100\% \quad (6)$$

where $\text{in}_{(s)}$ is the incidence at the middle of the canopy and $\text{re}_{(s)}$ is the reflection at the middle of the canopy.

2.3.3. Chlorophyll Content Index

In summer maize R1 and R2, chlorophyll content index (CCI) was measured using a CCM-200 Chlorophyll Content Meter (Opti-Sciences, Inc., Hudson, NH, USA). Three spiked leaves with uniform growth were selected from each plot [16].

2.3.4. Photosynthetic Parameters

The net photosynthetic rate (Pn) and transpiration rate (Tr) were measured using an LI-6400 Portable Photosynthetic Assay System (LI-COR, Lincoln, NE, USA). On a typical sunny day, Pn and Tr of the spike leaves of summer maize were measured between 9:00–11:00 a.m. Leaf water-use efficiency (WUE_L) was calculated as follows [51]:

$$\text{WUE}_\text{L} = \frac{\text{Pn}}{\text{Tr}} \quad (7)$$

where Pn is the net photosynthetic rate (μmol CO_2 m^{-2} s^{-1}) and Tr is the transpiration rate (mmol H_2O m^{-2} s^{-1}).

2.3.5. Dry-Matter Accumulation

At V6, V12, R1, R2, and R6 (mature stage) of summer maize, we selected representative plants from each plot, cut them into small samples, and placed them in an oven at 105 ºC for sterilization for 30 min. The samples were then dried to a constant weight at 85 °C. An electronic balance was used to weigh the dry-matter mass and calculate the dry-matter accumulation [49].

2.3.6. Radiation-Use Efficiency

The radiation-use efficiency (RUE) was calculated as the ratio of dry-matter accumulation to intercepted radiation during the growth periods. The daily solar radiation was recorded at an on-site weather station [16].

2.3.7. Grain Yield and Yield Components

In R6 of summer maize, 3 m double rows were selected in each plot for yield measurement. The number of spikes per unit area was calculated. After natural air drying, the number of rows per spike and grains per row was recorded. After threshing, an electronic balance was used to measure the yield and kernel weight and convert them to a mass containing 14% water [52].

2.4. Statistical Analysis

SPSS 26 (IBM, Chicago, IL, USA) data processing software was used for statistical analysis. An analysis of variance (ANOVA) was used to evaluate the differences between treatments. Differences were considered statistically significant at $p \leq 0.05$ according to the least significant difference (LSD).

3. Results

3.1. Leaf Area Index

Under each treatment, the LAI of summer maize showed a trend of rapid increase from V6 to R1, after which there was a gradual change (Figure 2). For the same genotype of summer maize, the LAI decreased with a reduction in planting density at every stage. The LAI under the ZH treatment was significantly higher than that of the other treatments. In both growing seasons, LAI was 15.71% higher in Zhengdan 958 than in Denghai 605.

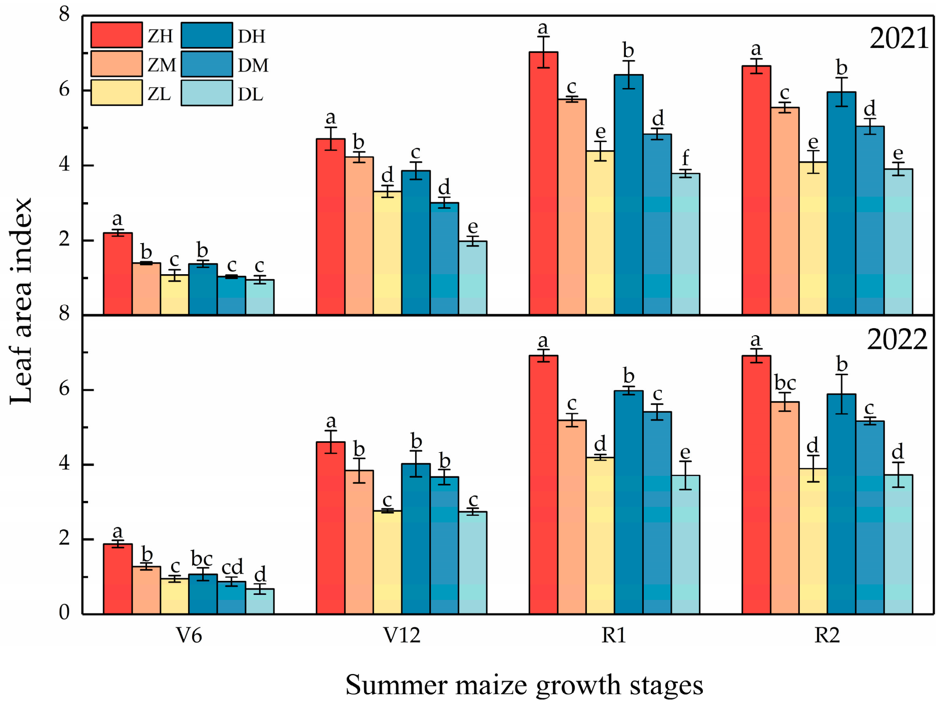

Figure 2. LAI of summer maize at different growing stages in the 2021 and 2022 summer maize growing seasons. Z represents Zhengdan 958, D represents Denghai 605; H represents high density, M represents middle density, and L represents low density. The measurement date was on 19 July, 27 July, 10 August, and 28 August, 2021; and 15 July, 27 July, 13 August, and 4 September, 2022, which belonged to V6 (the sixth-leaf stage), V12 (the twelfth-leaf stage), R1 (silking stage), and R2 (filling stage) of summer maize, respectively. Vertical bars represent standard errors. Bars labeled at the top of the column with different letters are significantly ($p < 0.05$) different among treatments using LSD post hoc test.

3.2. Photosynthetically Active Radiation

The PAR interception ratio of the canopy generally decreased with a decline in planting density during the summer maize R2 stage in 2021 and 2022 (Table 1). However, in both growing seasons, the PAR interception ratios of the H and M treatments were 6.70% and 4.66% higher on average than that of L, respectively. Meanwhile, in both growing seasons, the PAR penetration ratio of the canopy increased with the decrease in planting density, and the H and M treatments were significantly lower (52.61% and 32.81% on average, respectively) than L treatment.

The experimental year and planting density significantly interacted with the PAR interception ratio of the canopy. However, there were no significant interaction effects on the PAR interception ratio of the canopy between the other treatments.

Similar to the total canopy PAR interception ratio, both genotypes and planting densities significantly affected the PAR interception ratio in the middle of the canopy during the summer maize R2 stage in 2021 and 2022 (Figure 3). At the same density, the PAR interception ratio in the middle of the canopy of Zhengdan 958 was higher than that of Denghai 605. Compared with Denghai 605, the PAR interception ratio at the middle of the canopy under Zhengdan 958 treatments increased by 20.99%, 15.15%, and 9.82% for the H, M, and L conditions, respectively, in 2021, and 5.49%, 6.57%, and 7.61% in 2022, respectively. For the same genotype, the PAR interception ratio in the middle of the canopy is the highest under M treatment; however, no significant differences were found among the H and M treatments.

Table 1. Effects of planting densities and genotypes on canopy PAR interception ratio, penetration ratio, and reflection ratio during the summer maize R2 (filling stage) in 2021 and 2022.

Treatments	**Interception Ratio (%)**		**Penetration Ratio (%)**		**Reflection Ratio (%)**	
	2021	**2022**	**2021**	**2022**	**2021**	**2022**
Genotypes						
Z	89.02 [a]	92.65 [a]	7.82 [a]	5.67 [a]	3.16 [a]	1.68 [a]
D	88.69 [a]	90.63 [b]	7.88 [a]	7.58 [a]	3.43 [a]	1.79 [a]
p-value	0.854	0.046	0.964	0.072	0.602	0.520
Densities						
H	92.74 [a]	93.25 [a]	4.35 [c]	4.91 [b]	2.91 [b]	1.84 [a]
M	88.89 [b]	92.28 [a]	8.62 [b]	6.02 [b]	2.49 [b]	1.70 [b]
L	84.93 [c]	89.38 [b]	10.58 [a]	8.96 [a]	4.48 [a]	1.67 [c]
p-value	0.000	0.001	0.000	0.001	0.000	0.684
Treatments						
ZH	92.33 [a]	94.58 [a]	4.69 [c]	3.61 [d]	2.98 [b]	1.81 [a]
ZM	88.96 [b]	92.94 [ab]	8.97 [b]	5.46 [cd]	2.08 [b]	1.60 [a]
ZL	85.77 [bc]	90.43 [c]	9.79 [ab]	7.94 [ab]	4.44 [a]	1.63 [a]
DH	93.15 [a]	91.92 [bc]	4.01 [c]	6.20 [bc]	2.85 [b]	1.88 [a]
DM	88.82 [b]	91.63 [bc]	8.27 [b]	6.57 [bc]	2.91 [b]	1.80 [a]
DL	84.10 [c]	88.32 [d]	11.37 [a]	9.98 [a]	4.53 [a]	1.70 [a]
p-value	0.000	0.000	0.000	0.001	0.001	0.947
Interaction (*p*-value)						
Y × G	0.087		0.033		0.642	
Y × P	0.007		0.130		0.000	
G × P	0.568		0.294		0.375	
Y × G ×P	0.409		0.388		0.575	

The data were the average values on 12 September 2021 and 7 September 2022. Z represents Zhengdan 958, D represents Denghai 605; H represents high density, M represents middle density, L represents low density; Y represents experimental year, G represents genotypes, and P represents densities. In each growing season, in the same column, values followed by different letters differ significantly ($p < 0.05$) among treatments using LSD post hoc test.

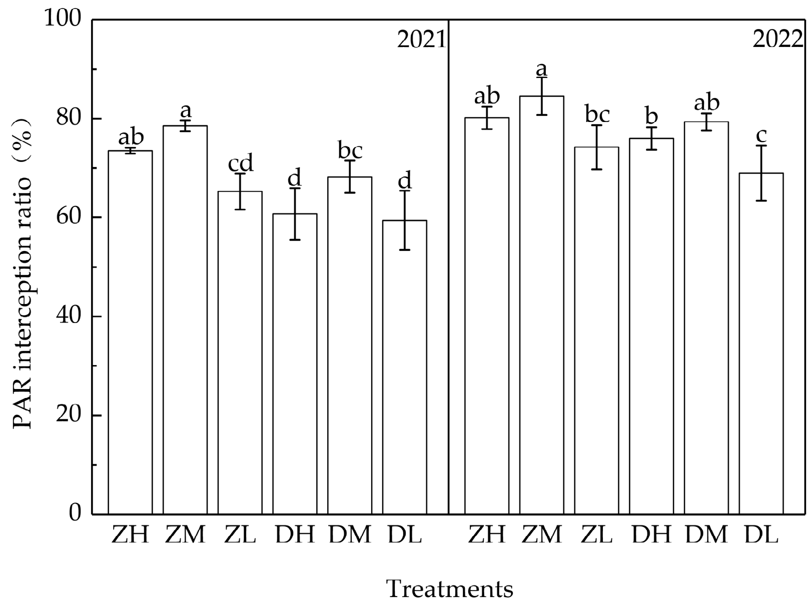

Figure 3. Effects of plant densities and genotypes on the PAR interception ratio at the middle of canopy at R2 (filling stage) in 2021 and 2022. Z represents Zhengdan 958, D represents Denghai 605; H represents high density, M represents middle density, and L represents low density. Vertical bars represent standard errors. Bars labeled at the top of the column with different letters are significantly ($p < 0.05$) different among treatments using LSD post hoc test.

3.3. Chlorophyll Content Index

The CCI of Denghai 605 was 28.17% and 17.03% higher than that of Zhengdan 958 in 2021 and 2022, respectively. Increasing planting density significantly diminished the CCI (Figure 4). Compared with the L treatment, at the R1 stage, CCI in M and H decreased by 3.32% and 6.30% in 2021 and by 8.34% and 14.60% in 2022, respectively; at the R2 stage, CCI in M and H decreased by 8.63% and 18.75% in 2021 and by 10.32% and 14.35% in 2022, respectively.

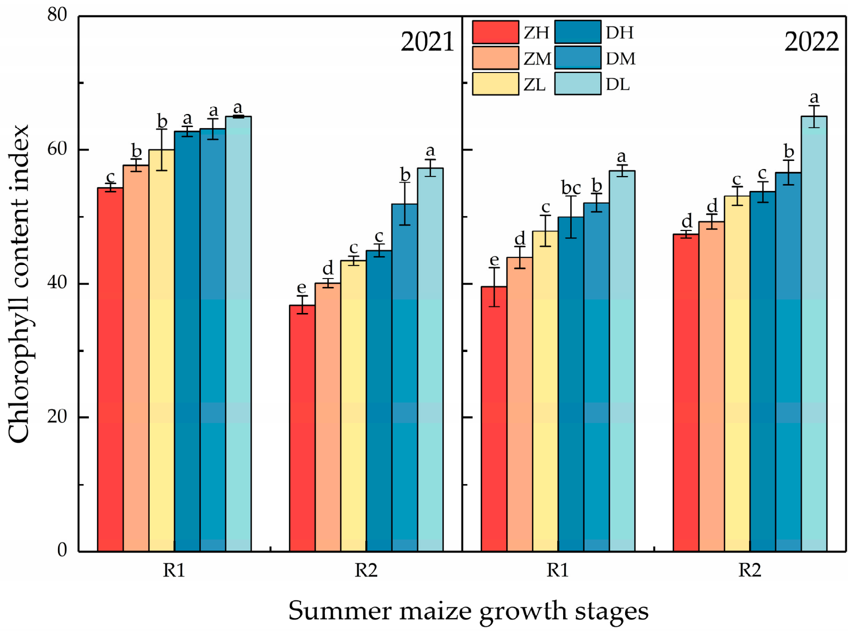

Figure 4. Effects of planting densities and genotypes on CCI at R1 (silking stage) and R2 (filling stage) in 2021 and 2022 summer maize growing seasons. Z represents Zhengdan 958, D represents Denghai 605; H represents high density, M represents middle density, and L represents low density. Vertical bars represent standard errors. Bars labeled at the top of the column with different letters are significantly ($p < 0.05$) different among treatments using LSD post hoc test.

3.4. Photosynthetic Parameters

In both growing seasons, the Pn of summer maize decreased with the increase in planting density. H and M treatments reduced the Pn of summer maize by 18.66% and 8.96% in the L treatments, respectively (Figure 5). Similar to Pn, the Tr of two genotypes for summer maize significantly decreased with the increasing planting density. The Tr of Denghai 605 was 27.45%, 16.14%, and 17.90% higher than that of Zhengdan 958 under H, M, and L conditions in 2021, respectively, and 23.62%, 5.18%, and 13.85% in 2022, respectively.

The higher the planting density, the larger the WUE_L of Zhengdan 958; however, the WUE_L of Denghai 605 is the highest in treatment M. The H treatment had the highest WUE_L, which was significantly higher than that of the other treatments during both growing seasons. For example, the WUE_L of Zhengdan 958 was 20.60% (2021) and 18.19% (2022) on average compared with Denghai 605; however, the significance appeared only in the H treatments.

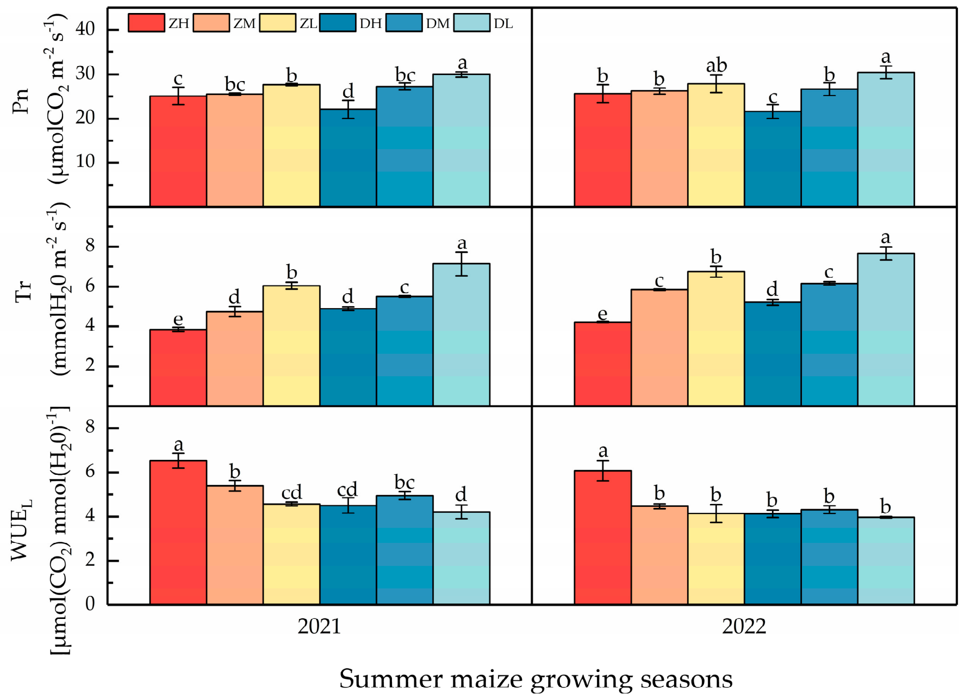

Figure 5. Effects of planting densities and genotypes on Pn, Tr, and WUE_L at R2 (filling stage) in 2021 and 2022 summer maize growing seasons. Z represents Zhengdan 958, D represents Denghai 605; H represents high density, M represents middle density, L represents low density. Vertical bars represent standard errors. Bars labeled at the top of the column with different letters are significantly ($p < 0.05$) different among treatments using LSD post hoc test.

3.5. Dry-Matter Accumulation and Radiation-Use Efficiency

In the vegetative stages (V6 and V12) and R1 of both growing seasons under the same planting density, the dry-matter accumulation of Zhengdan 958 was always higher than that of Denghai 605 (Figure 6). Under the same genotype conditions, the dry-matter accumulation in summer maize was in the order of H > M > L. During R6, the dry-matter accumulation under the DM treatment was the highest in both growth seasons, and it significantly increased by 16.31% compared with ZM in 2021.

Under the same genotype treatment, the RUE of the H treatment was the highest in the vegetative stages (V6–R1) of both growth seasons. In the reproductive stages (R1–R6) of both growing seasons, the RUE of the DM treatment was the highest, at 2.02 and 2.16 g MJ^{-1}, respectively (Figure 7). In both growing seasons, M planting density increased the RUE of summer maize by 10.61% and 25.76% for H and L, respectively, and the RUE of Denghai 605 was 18.19% higher on average than that of Zhengdan 958.

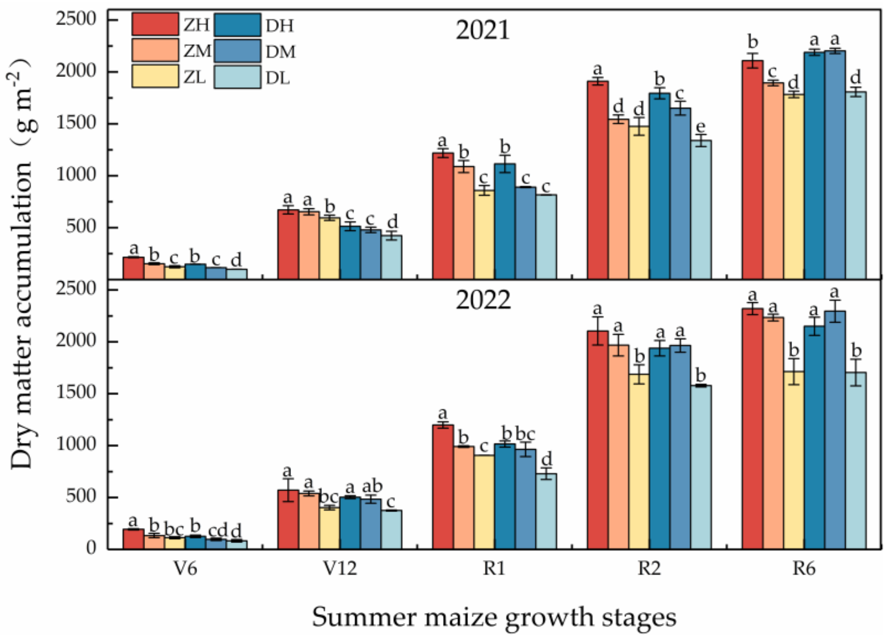

Figure 6. Effects of planting densities and genotypes on dry-matter accumulation at V6 (the sixth−leaf stage), V12 (the twelfth−leaf stage), R1 (silking stage), R2 (filling stage), and R6 (mature stage) in 2021 and 2022 summer maize growing seasons. Z represents Zhengdan 958, D represents Denghai 605; H represents high density, M represents middle density, and L represents low density. Vertical bars represent standard errors. Bars labeled at the top of the column with different letters are significantly (p < 0.05) different among treatments using LSD post hoc test.

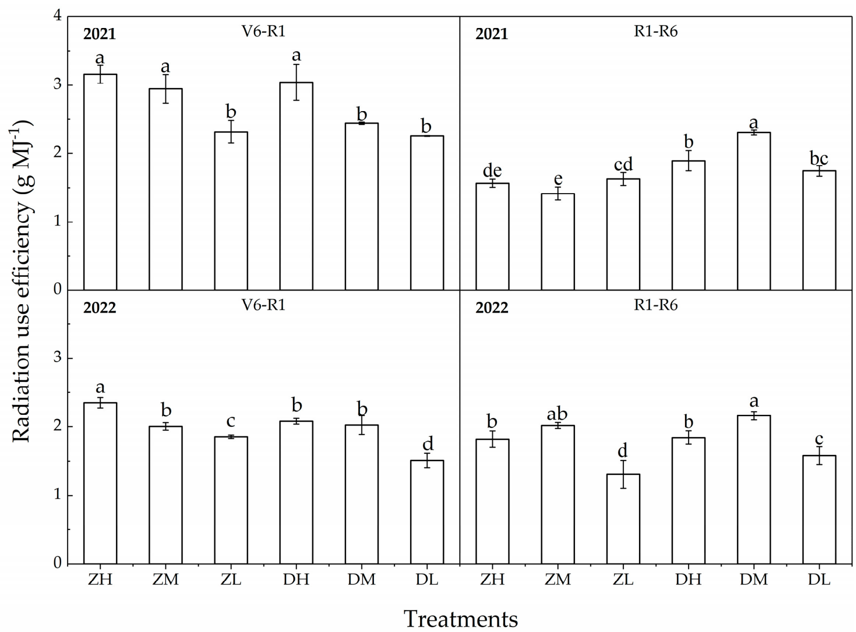

Figure 7. Effects of planting densities and genotypes between V6 (the sixth−leaf stage), R1 (silking stage), R1 (silking stage), R6 (mature stage) on radiation−use efficiency in 2021 and 2022 summer maize growing seasons. V6−R1 represents the stage from V6 to R1, R1−R6 represents the stage from R1 to R6; Z represents Zhengdan 958, D represents Denghai 605; H represents high density, M represents middle density, and L represents low density. Vertical bars represent standard errors. Bars labeled at the top of the column with different letters are significantly (p < 0.05) different among treatments using LSD post hoc test.

3.6. Grain Yield and Yield Components

The genotype significantly affected the number of rows per spike during both growing seasons. Rows per spike dramatically increased in Denghai 605 by 6.62% and 8.55% compared with Zhengdan 958 in 2021 and 2022, respectively (Table 2). Planting density significantly affected spike number, kernel number per row, 1000-kernel weight, and grain yield in summer maize. The spike number of summer maize under high-density treatment was significantly higher than that under medium-density (21.37% and 16.98%, respectively) and low-density (68.63% and 63.55%, respectively) treatments. However, the kernel numbers per row and 1000-kernel weight under the low-density treatment were higher than those under the high- and medium-density treatments. In 2021, the grain number per row at a low density and 1000-kernel weight at a high density significantly increased by 17.32% and 11.67% compared with medium- and high-density treatments, and by 21.16%, 18.45%, 8.07%, and 3.51%, respectively, compared with medium density. Although the increase in 1000-kernel weight under low density could compensate for the decrease in spike number, the yield under low density was significantly reduced by 26.86% and 24.83% compared with medium density in 2021 and 2022, respectively.

Table 2. Effects of planting density and genotypes on grain yield and yield components in 2021 and 2022 summer maize growing seasons.

Treatments	Spikes Numbers (Spikes m^{-2})		Rows Number per Spike (Rows Spike^{-1})		Kernel Numbers per Row (Kernels Row^{-1})		1000-Kernel Weight (g)		Grain Yield (t ha^{-1})	
	2021	2022	2021	2022	2021	2022	2021	2022	2021	2022
Genotypes										
Z	26.67 ^{a}	26.33 ^{a}	14.80 ^{b}	14.38 ^{b}	38.58 ^{a}	36.36 ^{a}	280.47 ^{a}	309.82 ^{a}	9.78 ^{a}	10.16 ^{a}
D	26.78 ^{a}	26.56 ^{a}	15.78 ^{a}	15.61 ^{a}	36.45 ^{a}	34.62 ^{a}	293.60 ^{a}	314.70 ^{a}	10.08 ^{a}	10.15 ^{a}
p-value	0.969	0.933	0.003	0.000	0.160	0.252	0.131	0.682	0.630	0.984
Densities										
H	33.17 ^{a}	32.17 ^{a}	15.10 ^{a}	15.00 ^{a}	34.46 ^{c}	31.95 ^{c}	267.06 ^{b}	281.42 ^{c}	9.95 ^{b}	10.06 ^{b}
M	27.33 ^{b}	27.50 ^{b}	15.17 ^{a}	14.73 ^{a}	37.73 ^{b}	35.82 ^{b}	295.99 ^{a}	322.02 ^{b}	11.10 ^{a}	11.52 ^{a}
L	19.67 ^{c}	19.67 ^{c}	15.60 ^{a}	15.25 ^{a}	40.43 ^{a}	38.71 ^{a}	298.06 ^{a}	333.33 ^{a}	8.75 ^{c}	8.89 ^{c}
p-value	0.000	0.000	0.506	0.569	0.001	0.000	0.001	0.000	0.002	0.000
Treatments										
ZH	32.67 ^{a}	32.00 ^{a}	15.13 ^{bc}	14.40 ^{c}	36.50 ^{b}	32.73 ^{cd}	261.78 ^{d}	286.70 ^{d}	10.48 ^{ab}	10.66 ^{b}
ZM	27.67 ^{b}	27.00 ^{b}	14.73 ^{c}	14.33 ^{c}	38.70 ^{ab}	37.00 ^{b}	297.46 ^{b}	316.59 ^{c}	11.02 ^{a}	11.11 ^{ab}
ZL	19.67 ^{c}	20.00 ^{c}	14.53 ^{c}	14.40 ^{c}	40.55 ^{a}	39.37 ^{a}	282.17 ^{c}	276.14 ^{e}	7.84 ^{c}	8.72 ^{c}
DH	33.67 ^{a}	32.33 ^{a}	15.07 ^{bc}	15.60 ^{ab}	32.42 ^{c}	31.18 ^{d}	272.34 ^{c}	326.17 ^{b}	9.43 ^{b}	9.46 ^{c}
DM	27.00 ^{b}	28.00 ^{b}	16.47 ^{a}	15.13 ^{bc}	36.75 ^{b}	34.63 ^{c}	294.51 ^{b}	327.45 ^{b}	11.17 ^{a}	11.94 ^{a}
DL	19.67 ^{c}	19.33 ^{c}	15.80 ^{ab}	16.10 ^{a}	40.21 ^{a}	38.05 ^{ab}	313.96 ^{a}	340.50 ^{a}	9.65 ^{b}	9.05 ^{c}
p-value	0.000	0.000	0.002	0.003	0.001	0.000	0.000	0.000	0.001	0.000
Interaction (*p*-value)										
Y × G	0.894		0.417		0.694		0.032		0.436	
Y × P	0.469		0.045		0.764		0.000		0.778	
G × P	0.618		0.059		0.244		0.000		0.001	
Y × G × P	0.423		0.025		0.292		0.001		0.113	

Z represents Zhengdan 958, D represents Denghai 605; H represents high density, M represents middle density, L represents low density; Y represents experimental year, G represents genotypes and P represents densities. In each growing season, in the same column, values followed by different letters differ significantly ($p < 0.05$) among treatments using LSD post hoc test.

Significant interactions were found between genotype and planting density for grain yield. However, neither the experimental years and genotypes or the experimental years and densities had a significant interaction effect on grain yield. Additionally, there was no three-way interaction impact between density, genotype, and experimental year.

4. Discussion

In the present study, the LAI of summer maize increased with increasing planting density (Figure 2). As the summer maize density increases, competition among plants intensifies and, consequently, maize leaves may develop rapidly, resulting in a larger LAI [53]. In addition, the effective number of plants per unit area is an important reason for the increase in LAI. Therefore, our results are in agreement with those reported by Gou et al. [54].

The fluctuations in the overall canopy's PAR interception ratio were consistent with LAI, which showed an increasing tendency with improved planting density (Table 1). However, the PAR interception ratio in the middle of the canopy under the medium-density treatment was higher than that under high- and low-density treatments (Figure 3). Higher LAI aggravated the shading effects between summer maize plants under high-density treatment, significantly reducing the PAR interception ratio measured at the middle and bottom of the canopy, thereby reducing the photosynthetic capacity of leaves located at the bottom of the canopy [53,55]. Liu et al. [56] found that with an increase in plant density, the amount of solar radiation intercepted by the lower leaves decreased and the leaf senescence speed increased, which agrees with our study. Moreover, the PAR interception ratio at the middle of the canopy significantly impacted the grain yield because the spiked leaf and its adjacent leaves are the most vital functions in the grain formation of summer maize [57]. Chen et al. [58] found that the overgrowth of crop vegetation increased the shading of leaves, thus reducing PAR conversion efficiency, which is consistent with our results. Therefore, we conclude that for summer maize with high-density treatment, the transmittance of PAR in the canopy decreases because of the larger canopy LAI, resulting in an uneven distribution of PAR in the canopy. Therefore, dry-matter accumulation in summer maize decreases, slowing the transport of photosynthetic substances to the grain.

In this study, the genotypes of summer maize had a significant impact on CCI. Electron transfer in cells mainly depends on chlorophyll molecules, and can control how light energy is absorbed, transformed, and distributed. They also contribute to photosynthesis [59,60]. A higher CCI can delay leaf senescence and improve filling efficiency [17]. Cellular aging causes cellular proteins to break down and Pn levels to drop, thus decreasing Pn [61]. For example, Li et al. [62] found that CCI was closely related to the yield of summer maize. The CCI of Denghai 605 was higher than that of Zhengdan 958, which improved the photosynthetic performance of Denghai 605, promoted the transformation of dry matter into grains, and increased the yield of Denghai 605.

Pn and Tr are the highest in low density because, as the planting density of summer maize decreased, the biomass and activity of the root system of a single plant increased [63]. As a result, the root could absorb more soil moisture and increase soil water-use efficiency [64]. Water strongly controls the growth of crops [65]. The root system's capacity to take in and transmit water is enhanced with an increase in Tr [66]. A better water environment could optimize Pn and Tr [67], promote the synthesis of chlorophyll, and reduce the degradation of chlorophyll, and the increase in Pn could react with CCI and enhance the photosynthetic performance of leaves [68]. Therefore, with an increase in Pn, the photosynthetic performance of summer maize was enhanced, and the efficiency of transforming photosynthetic effective radiation into dry-matter accumulation was also improved. In the 2021 and 2022 growing seasons, the Pn of the DH treatment was lower than that of the ZH treatment in R2. This indicated that the conversion efficiency of the DH treatment to dry-matter accumulation through photosynthetic active radiation was lower than that of the ZH treatment, resulting in a lower yield of the DH treatment than that of the ZH treatment. In addition, the WUE_L of Zhengdan 958 increased when the planting density increased. However, the WUE_L of Denghai 605 was the highest under the medium-density treatment. Crop transpiration was the main component of water consumption [69]. Although photosynthesis was lower in Zhengdan 958 under the high-density treatment, transpiration was also minimal, leading to a higher WUE_L.

During R2, the dry-matter accumulation of summer maize was the highest at a medium planting density (except for the ZM treatment in 2021, and no significant differences were found between ZM and ZH). This was because the accumulation of dry matter mainly depended on the interception of solar radiation and the use of radiant energy [70,71]. The intercepted quantity of PAR in maize leaves under the low-density treatment was low, leading to a lower dry-matter accumulation. However, under high-density treatment, the weak light caused by shading obstructed electron transmission in plants, reducing the photosynthetic efficiency of summer maize [72]. Finally, dry-matter accumulation in the late R2 of summer maize was relatively slow. A higher planting density of summer maize could improve the dry-matter accumulation and grain yield per area and increase the competition for environmental resources among single-summer maize [73]. Therefore, dry-matter accumulation in summer maize was highest under the medium planting density treatment.

In this study, low planting density increased the 1000-grain weight of summer maize but decreased the spike number in relation to medium and high planting density. The reduction in spike number was due to the decline in effective plants per unit area caused by planting density, which reduced the spike number of summer maize and reduced yield. Yan et al. [74] also demonstrated that crop yield under low-density treatments was positively correlated based on the quantity of panicles per square inch. The 1000-grain weight at a high density was less than that at medium and low densities. This result was consistent with that of Liu et al. [75], who found that high-density planting would reduce the 1000-grain weight by 4–8%. The decrease in the 1000-grain weight under high-density treatment was due to competition between limited water and nutrition [76]. Similarly, the decrease in grain number per row was also a key factor in the reduction in yield under high planting density. However, the increase in the number of spikes under the high-density planting pattern could not compensate for the decrease in the 1000-grain weight and grain number per spike [77]. The soil nutrients might not be fully supplied to satisfy the growth needs of maize with increasing planting density, and the lack of effective light resources and carbohydrate assimilation of a single plant leads to a lower yield under high-density planting patterns than that of medium- and low-density planting patterns [78]. A similar study was reported by Testa et al. [79], who found that high-density planting (10 plants m^{-2}) influences the development of grains and decreases the yield potential of a single plant.

There were only two summer maize genotypes designed in this experiment. Considering that different genotypes may have different agronomic characters, thus affecting RUE, we need to design experiments using more genotypes to verify our ideas. Taking the differences in soil temperature into account, the different planting density is likely to affect it; therefore, further research is necessary to determine whether this affects the efficiency of radiation used by summer maize.

5. Conclusions

In the present study, we investigated the response of the RUE and WUE_L of summer maize to planting densities and genotypes in the NCP. The LAI and canopy PAR interception ratio decreased with reductions in planting density. The effective radiation interception rate in the middle of the canopy, RUE, and yield were the highest under 78,000 plants ha^{-1}. The average RUE of Denghai 605 was 18.19% higher than that of Zhengdan 958. Planting density had a significant effect on yield and yield components. The 1000-kernel weight at low density was higher but could not compensate for the decrease in spike number; therefore, the yield at low density was significantly reduced by 25.85% compared with that at medium density. The drought-resistant genotype (Zhengdan 958) increased WUE_L by 19.45% compared with the drought-sensitive genotype (Denghai 605), and under high planting density, it was high. Although the WUE_L of Zhengdan958 was high, owing to the relatively low Tr level, the grain yield and RUE at R2 were lower. In summary, Denghai 605 with a density of 78,000 plants ha^{-1} had the highest RUE and summer maize yield in the NCP. Therefore, we recommend using Denghai605 with a planting density of 78,000 plants ha^{-1} in the NCP for maintaining a stable grain yield of summer maize. Further studies are needed to prove the molecular mechanism of planting density and genotype on the high photosynthetic efficiency of summer maize.

Author Contributions: Writing—review and editing, Z.L. and R.Z.; writing—original draft preparation, Z.L. and R.Z.; methodology, Q.Z. and S.W.; data curation, M.L. and S.W.; software, Z.L. and Q.L.; resources, Q.L.; funding acquisition, Q.L.; conceptualization, Z.L. and Q.Z.; investigation, M.L. and R.Z. All authors have read and agreed to the published version of the manuscript.

Funding: This research was funded by the Key Research and Development Plan in Shandong Province, China (2019GSF109054).

Data Availability Statement: The datasets used and/or analyzed during the current study are available from the corresponding author upon reasonable request.

Conflicts of Interest: The authors declare no conflict of interest.

References

1. Goncharova, N.A.; Merzlyakova, N.V. Food shortages and hunger as a global problem. *Food Sci. Technol.* **2022**, *42*, e70621. [CrossRef]
2. Chen, Z.Y.; Huang, W.; Ma, L.J.; Xu, H.; Cheng, Y.H. Application and development of big data in sustainable utilization of soil and land resources. *IEEE Access* **2020**, *8*, 152751–152759. [CrossRef]
3. Erenstein, O.; Jaleta, M.; Sonder, K.; Mottaleb, K.; Prasanna, B.M. Global maize production, consumption and trade: Trends and R&D implications. *Food Secur.* **2022**, *14*, 1295–1319.
4. Tan, D.C.; Fan, Y.L.; Liu, J.M.; Zhao, J.T.; Ma, Y.Z.; Li, Q.Q. Winter wheat grain yield and quality response to straw mulching and planting pattern. *Agric. Res.* **2019**, *8*, 548–552. [CrossRef]
5. Kang, S.Z.; Hao, X.M.; Du, T.S.; Tong, L.; Sun, X.L.; Lu, H.N.; Li, X.L.; Huo, Z.L.; Li, S.E.; Ding, R.S. Improving agricultural water productivity to ensure food security in China under changing environment: From research to practice. *Agric. Water Manag.* **2018**, *179*, 5–17. [CrossRef]
6. Du, T.S.; Kang, S.Z.; Zhang, J.H.; Davies, W.J. Deficit irrigation and sustainable water-resource strategies in agriculture for China's food security. *J. Exp. Bot.* **2015**, *66*, 2253–2269. [CrossRef]
7. Xue, J.; Xie, R.Z.; Zhang, W.F.; Wang, K.R.; Hou, P.; Ming, B.; Gou, L.; Li, S.K. Research progress on reduced lodging of high-yield and -density maize. *J. Integr. Agric.* **2017**, *16*, 2717–2725. [CrossRef]
8. Li, G.H.; Cheng, Q.; Li, L.; Lu, D.L.; Lu, W.P. N, P and K use efficiency and maize yield responses to fertilization modes and densities. *J. Integr. Agric.* **2021**, *20*, 78–86. [CrossRef]
9. Zhao, C.H.; Ji, S.W.; Ge, C.; Su, Y.J.; Shi, Z.X.; Cui, Z.H.; Zhang, A.; Wang, Z.Y.; Ruan, Y.Y.; Zhang, L.J.; et al. Transcriptional analyses of maize leaves in response to high-density planting. *Agron. J.* **2022**, *114*, 1385–1400. [CrossRef]
10. Ma, X.Y.; He, Q.J.; Zhou, G.S. Sequence of changes in maize responding to soil water deficit and related critical thresholds. *Front. Plant Sci.* **2018**, *9*, 511. [CrossRef]
11. Gu, X.B.; Cai, H.J.; Fang, H.; Chen, P.P.; Li, Y.P.; Li, Y.N. Soil hydro-thermal characteristics, maize yield and water use efficiency as affected by different biodegradable film mulching patterns in a rain-fed semi-arid area of China. *Agric. Water Manag.* **2021**, *245*, 106560. [CrossRef]
12. Qasemipour, E.; Abbasi, A. Assessment of agricultural water resources sustainability in arid regions using virtual water concept: Case of South Khorasan Province, Iran. *Water* **2019**, *11*, 3. [CrossRef]
13. Kummu, M.; Fader, M.; Gerten, D.; Guillaume, J.H.A.; Jalava, M.; Jagermeyr, J.; Pfister, S.; Porkka, M.; Siebert, S.; Varis, O. Bringing it all together: Linking measures to secure nations' food supply. *Curr. Opin. Environ. Sustain.* **2017**, *29*, 98–117. [CrossRef]
14. Magalhaes, M.D.; Martuscello, J.A.; da Fonseca, D.M.; de Oliveira, I.M.; de Freitas, F.P.; Faria, D.J.G.; de Oliveira, R.A.; Ribeiro, J.I. 2012. Morphogenesis and structural characteristics and production of guinea grass irrigated under different plants density and nitrogen doses. *Rev. Bras. Zootecn.* **2012**, *40*, 2308–2317.
15. Lal, M.K.; Sharma, N.; Adavi, S.B.; Sharma, E.; Altaf, M.A.; Tiwari, R.K.; Kumar, R.; Kumar, A.; Dey, A.; Paul, V. From source to sink: Mechanistic insight of photoassimilates synthesis and partitioning under high temperature and elevated [CO_2]. *Plant Mol.Biol.* **2022**, *110*, 305–324. [CrossRef]
16. Jiao, F.L.; Hong, S.Z.; Liu, C.Y.; Ma, Y.Z.; Zhang, M.M.; Li, Q.Q. Wide-precision planting pattern under different tillage methods affects photosynthesis and yield of winter wheat. *Arch. Agron. Soil Sci.* **2021**, *68*, 1352–1368. [CrossRef]
17. Hafeez, A.; Ali, S.; Ma, X.L.; Tung, S.A.; Shah, A.N.; Ahmad, S.; Chattha, M.S.; Souliyanonh, B.; Zhang, Z.; Yang, G.Z. Photosynthetic characteristics of boll subtending leaves are substantially influenced by applied K to N ratio under the new planting model for cotton in the Yangtze River Valley. *Field Crop. Res.* **2019**, *237*, 43–52. [CrossRef]
18. Huang, M.; Shan, S.L.; Zhou, X.F.; Chen, J.N.; Cao, F.B.; Jiang, L.G.; Zou, Y.B. Leaf photosynthetic performance related to higher radiation use efficiency and grain yield in hybrid rice. *Field Crop. Res.* **2016**, *193*, 87–93. [CrossRef]

19. Zhao, W.S.; Sun, Y.L.; Kjelgren, R.; Liu, X.P. Response of stomatal density and bound gas exchange in leaves of maize to soil water deficit. *Acta Physiol. Plant.* **2015**, *37*, 1704. [CrossRef]
20. Uddin, S.; Parvin, S.; Low, M.; Fitzgerald, G.J.; Tausz-Posch, S.; Armstrong, R.; Tausz, M. Water use dynamics of dryland canola (*Brassica napus* L.) grown on contrasting soils under elevated CO_2. *Plant Soil* **2019**, *438*, 205–222. [CrossRef]
21. Ren, B.; Zhang, J.; Dong, S.; Liu, P.; Zhao, B. Effects of duration of waterlogging at different growth stages on grain growth of summer maize (*Zea mays* L.) under field conditions. *J. Agron. Crop Sci.* **2016**, *202*, 564–575. [CrossRef]
22. Gao, J.; Shi, J.G.; Dong, S.T.; Liu, P.; Zhao, B.; Zhang, J.W. Grain development and endogenous hormones in summer maize (*Zea mays* L.) submitted to different light conditions. *Int. J. Biometeorol.* **2018**, *62*, 2131–2138. [CrossRef] [PubMed]
23. Yang, Y.S.; Liu, G.Z.; Guo, X.X.; Liu, W.M.; Xue, J.; Ming, B.; Xie, R.Z.; Wang, K.R.; Hou, P.; Li, S.K. Quantitative Relationship Between Solar Radiation and Grain Filling Parameters of Maize. *Front. Plant Sci.* **2022**, *13*, 906060. [CrossRef] [PubMed]
24. Wang, J.; Shi, K.; Lu, W.P.; Lu, D.L. Effects of post-silking shading stress on enzymatic activities and phytohormone contents during grain development in spring maize. *J. Plant Growth Regul.* **2020**, *40*, 1060–1073. [CrossRef]
25. Bellasio, C.; Griffiths, H. Acclimation of C-4 metabolism to low light in mature maize leaves could limit energetic losses during progressive shading in a crop canopy. *J. Exp. Bot.* **2014**, *65*, 3725–3736. [CrossRef]
26. Li, L.H.; Zhang, Y.P.; You, G.Y.; Yao, Y.G.; Tan, Z.H.; Song, Q.H.; Luo, Y.Y. Spatiotemporal distribution pattern of photosynthetically active radiation in subtropical evergreen broadleaved forest in Ailaoshan Mountains of Southwest China. *Chin. J. Ecol.* **2011**, *30*, 2394–2399.
27. Wang, Q.R.; Chen, H.X.; Han, Y.C.; Xing, F.F.; Wang, Z.B.; Feng, L.; Wang, G.P.; Yang, B.F.; Lei, Y.P.; Xiong, S.W.; et al. Effect of spatial-temporal light competition on cotton yield and yield distribution. *Agronomy* **2021**, *11*, 2346. [CrossRef]
28. Asilevi, P.; Quansah, E.; Dogbey, F. Satellite-based estimates of photosynthetically active radiation for tropical ecosystems in Ghana-West Africa. *Trop. Ecol.* **2022**, *63*, 615–625.
29. Zhao, D.D.; Shen, J.Y.; Lang, K.; Liu, Q.R.; Li, Q.Q. Effects of irrigation and wide-precision planting on water use, radiation interception, and grain yield of winter wheat in the North China Plain. *Agric. Water Manag.* **2013**, *118*, 87–92.
30. Monteith, J.L.; Moss, C.J. Climate and the efficiency of crop production in Britain. *Philos. Trans. R. Soc. B Biol. Sci.* **1977**, *281*, 277–294.
31. Perez, C.M.; Ayala, C.R.; Ruiz, A.M.; Bustamante, W.O.; Islas, J.D.R.; Hernandez, R.A.; Ordaz, A.L.; Ramirez, F.N. Leaf area and its impact in yield and quality of greenhouse tomato (*Solanum lycopersicum* L.). *Rev. Fac. Cienc. Agrar. Univ. Nac. Cuyo.* **2022**, *54*, 57–69.
32. Whitfield, D.M.; Smith, C.J. Effects of irrigation and nitrogen on growth, light interception and efficiency of light conversion in wheat. *Field Crop. Res.* **1989**, *20*, 279–295. [CrossRef]
33. Liu, W.M.; Hou, P.; Liu, G.Z.; Yang, Y.S.; Guo, X.X.; Ming, B.; Xie, R.Z.; Wang, K.R.; Liu, Y.E.; Li, S.K. Contribution of total dry matter and harvest index to maize grain yield-A multisource data analysis. *Food Energy Secur.* **2020**, *9*, e256. [CrossRef]
34. Zhou, H.L.; Zhou, G.S.; Zhou, L.; Lv, X.M.; Ji, Y.H.; Zhou, M.Z. The interrelationship between water use efficiency and radiation use efficiency under progressive soil drying in maize. *Front. Plant Sci.* **2022**, *12*, 794409. [CrossRef]
35. Drewry, D.T.; Kumar, P.; Long, S.P. Simultaneous improvement in productivity, water use, and albedo through crop structural modification. *Glob. Change Biol.* **2014**, *20*, 1955–1967. [CrossRef]
36. Leakey, A.D.B.; Ferguson, J.N.; Pignon, C.P.; Wu, A.; Jin, Z.N.; Hammer, G.L.; Lobell, D.B. Water use efficiency as a constraint and target for improving the resilience and productivity of C-3 and C-4 crops. *Annu. Rev. Plant Biol.* **2019**, *70*, 781–808. [CrossRef]
37. Gao, X.Y.; Li, C.; Cai, Y.; Ye, L.; Xiao, L.D.; Zhou, G.M.; Zhou, Y.F. Influence of scale effect of canopy projection on understory microclimate in three subtropical urban broad-leaved forests. *Remote Sens.* **2021**, *13*, 3786. [CrossRef]
38. Kim, D.S.; Marshall, E.J.P.; Brain, P.; Casseley, J.C. Effects of crop canopy structure on herbicide deposition and performance. *Weed Res.* **2011**, *51*, 310–320. [CrossRef]
39. Li, J.; Xie, R.Z.; Wang, K.R.; Hou, P.; Ming, B.; Zhang, G.Q.; Liu, G.Z.; Wu, M.; Yang, Z.S.; Li, S.K. Response of canopy structure, light interception and grain yield to plant density in maize. *J. Agric. Sci.* **2018**, *156*, 785–794. [CrossRef]
40. Liang, Q.; Shi, X.J.; Li, N.N.; Shi, F.; Tian, Y.; Zhang, H.X.; Hao, X.Z.; Luo, H.H. Fertilizer reduction combined with organic liquid fertilizer improved canopy structure and function and increased cotton yield. *Agronomy* **2022**, *12*, 1759. [CrossRef]
41. Bailey, B.N.; Fu, K.M. The probability distribution of absorbed direct, diffuse, and scattered radiation in plant canopies with varying structure. *Agric. For. Meteorol.* **2022**, *322*, 109009. [CrossRef]
42. Yu, N.N.; Ren, B.Z.; Zhao, B.; Liu, P.; Zhang, J.W. Optimized agronomic management practices narrow the yield gap of summer maize through regulating canopy light interception and nitrogen distribution. *Eur. J. Agron.* **2022**, *137*, 126520. [CrossRef]
43. Shi, D.Y.; Li, Y.H.; Zhang, J.W.; Liu, P.; Zhao, B.; Dong, S.T. Increased plant density and reduced N rate lead to more grain yield and higher resource utilization in summer maize. *J. Integr. Agric.* **2016**, *15*, 2515–2528. [CrossRef]
44. Chen, Z.J.; Sun, S.J.; Zhu, Z.C.; Jiang, H.; Zhang, X.D. Assessing the effects of plant density and plastic film mulch on maize evaporation and transpiration using dual crop coefficient approach. *Agric. Water Manag.* **2019**, *225*, 105765. [CrossRef]
45. Liu, T.N.; Gu, L.M.; Dong, L.M.; Zhang, J.W.; Liu, P.; Zhao, B. Optimum leaf removal increases canopy apparent photosynthesis, C–13–photosynthate distribution and grain yield of maize crops grown at high density. *Field Crop. Res.* **2015**, *170*, 32–39. [CrossRef]

46. Xu, W.J.; Liu, C.W.; Wang, K.R.; Xie, R.Z.; Ming, B.; Wang, Y.H.; Zhang, G.Q.; Liu, G.Z.; Zhao, R.L.; Fan, P.P.; et al. Adjusting maize plant density to different climatic conditions across a large longitudinal distance in China. *Field Crop. Res.* **2017**, *212*, 126–134. [CrossRef]
47. Kiniry, J.R.; Bean, B.; Xie, Y.; Chen, P.Y. Maize yield potential: Critical processes and simulation modeling in a high-yielding environment. *Agric. Syst.* **2004**, *82*, 45–56. [CrossRef]
48. Shi, D.Y.; Huang, Q.W.; Liu, Z.J.; Liu, T.; Su, Z.E.; Guo, S.B.; Bai, F.; Sun, S.; Lin, X.M.; Li, T.; et al. Radiation use efficiency and biomass production of maize under optimal growth conditions in Northeast China. *Sci. Total Environ.* **2022**, *836*, 155574. [CrossRef] [PubMed]
49. Liu, J.M.; Fan, Y.L.; Ma, Y.Z.; Li, Q.Q. Response of photosynthetic active radiation interception, dry matter accumulation, and grain yield to tillage in two winter wheat genotypes. *Arch. Agron. Soil Sci.* **2020**, *66*, 1103–1114. [CrossRef]
50. Sun, R.; Peng, C.; Cong, Y.X. Dynamic characteristics of leaf area index and their effects on yield in different density spring-maize. *J. Maize Sci.* **2008**, *16*, 61–65.
51. Fan, Y.L.; Liu, J.M.; Zhao, J.T.; Ma, Y.Z.; Li, Q.Q. Effects of delayed irrigation during the jointing stage on the photosynthetic characteristics and yield of winter wheat under different planting patterns. *Agric. Water Manag.* **2019**, *221*, 371–376. [CrossRef]
52. Ma, Y.Z.; Zhang, H.; Xue, Y.F.; Gao, Y.B.; Qian, X.; Dai, H.C.; Liu, K.C.; Li, Q.Q.; Li, Z.X. Effect of sulfur fertilizer on summer maize grain yield and soil water utilization under different irrigation patterns from anthesis to maturity. *Agric. Water Manag.* **2021**, *250*, 106828. [CrossRef]
53. Xue, J.; Guo, L.; Shi, Z.G.; Zhao, Y.S.; Zhang, W.F. Effect of leaf removal on photosynthetically active radiation distribution in maize canopy and stalk strength. *J. Integr. Agric.* **2017**, *16*, 85–96. [CrossRef]
54. Gou, L.; Xue, J.; Qi, B.Q.; Ma, B.Y.; Zhang, W.F. Morphological variation of maize cultivars in response to elevated plant densities. *Agron. J.* **2017**, *109*, 1443–1453. [CrossRef]
55. Xue, J.; Zhao, Y.S.; Gou, L.; Shi, Z.G.; Yao, M.N.; Zhang, W.F. How high plant density of maize affects basal internode development and strength formation. *Crop. Sci.* **2016**, *56*, 3295–3306. [CrossRef]
56. Liu, T.N.; Wang, Z.L.; Cai, T. Canopy apparent photosynthetic characteristics and yield of two spike-type wheat cultivars in response to row spacing under high plant density. *PLoS One* **2016**, *11*, e0148582. [CrossRef]
57. Bai, Y.X.; Wang, Z.R.; Zhong, G. Analysis on characters of three ear leaves of parents of high combining ability and hybrids of corn and correlative research of leaf area. *J. Maize Sci.* **1999**, *7*, 24–26.
58. Chen, Y.H.; Yu, S.L.; Yu, Z.W. Relationship between amount or distribution of PAR interception and grain output of wheat communities. *Acta Agron. Sin.* **2003**, *29*, 730–734.
59. Hortensteiner, S.; Krautler, B. Chlorophyll breakdown in higher plants. *Biochim. Biophys. Acta-Bioenerg* **2011**, *1807*, 977–988. [CrossRef]
60. Shanmugam, S.; Xu, J.T.; Boyer, C. Utilizing the electron transfer mechanism of chlorophyll a under light for controlled radical polymerization. *Chem. Sci.* **2015**, *6*, 1341–1349. [CrossRef]
61. He, J.N.; Shi, Y.; Zhao, J.Y.; Yu, Z.W. Strip rotary tillage with subsoiling increases winter wheat yield by alleviating leaf senescence and increasing grain filling. *Crop. J.* **2019**, *8*, 327–340. [CrossRef]
62. Li, H.J.; Kuang, N.K.; Gou, Q.S.; Ma, Y.Z.; Li, Q.Q. Effects of different film mulches on photosynthetic characteristics and yield of summer maize (*Zea mays* L.) in the North China Plain. Arch. *Agron. Soil Sci.* **2020**, *67*, 179–190. [CrossRef]
63. Shao, H.; Shi, D.F.; Shi, W.J.; Ban, X.B.; Chen, Y.C.; Ren, W.; Chen, F.J.; Mi, G.H. Genotypic difference in the plasticity of root system architecture of field-grown maize in response to plant density. *Plant Soil* **2019**, *439*, 201–217. [CrossRef]
64. Xu, J.; Guo, Z.Y.; Li, Z.M.; Li, F.J.; Xue, X.K.; Wu, X.R.; Zhang, X.M.; Li, H.; Zhang, X.D.; Han, Q.F. Stable oxygen isotope analysis of the water uptake mechanism via the roots in spring maize under the ridge-furrow rainwater harvesting system in a semi-arid region. *Agric. Water Manag.* **2021**, *252*, 106879. [CrossRef]
65. Chen, S.; Mao, X.M.; Shang, S.H. Response and contribution of shallow groundwater to soil water/salt budget and crop growth in layered soils. *Agric. Water Manag.* **2022**, *266*, 107574. [CrossRef]
66. Hayat, F.; Ahmed, M.A.; Zarebanadkouki, M.; Javaux, M.; Cai, G.C.; Carminati, A. Transpiration reduction in maize (*Zea mays* L) in response to soil drying. *Front. Plant Sci.* **2020**, *10*, 1695. [CrossRef]
67. Xu, J.; He, Z.K.; Feng, Q.Q.; Zhang, Y.Y.; Li, X.S.; Xu, J.J.; Lin, X.; Han, H.F.; Ning, T.Y.; Li, Z.J. Effect of tillage method on photosynthetic characteristics and annual yield formation of winter wheat-summer maize cropping system. *Plant Nutr. Fertil. Sci.* **2017**, *23*, 10–109.
68. Jiao, F.L.; Hong, S.Z.; Zhang, Q.F.; Li, M.; Shi, R.L.; Ma, Y.Z.; Li, Q.Q. Subsoiling before winter wheat cultivation increases photosynthetic characteristics and leaf water-use efficiency of summer maize in a double-cropping system. *Arch. Agron. Soil Sci.* **2022**, *269*, 107685. [CrossRef]
69. Jin, X.X.; Zuo, Q.; Ma, W.W.; Li, S.; Shi, J.C.; Tao, Y.Y.; Zhang, Y.A.; Liu, Y.; Liu, X.F.; Liu, S.; et al. Water consumption and water-saving characteristics of a ground cover rice production system. *J. Hydrol.* **2016**, *540*, 220–231. [CrossRef]
70. Honnaiah, P.A.; Sridhara, S.; Gopakkali, P.; Ramesh, N.; Mahmoud, E.A.; Abdelmohsen, S.A.M.; Alkallas, F.H.; El-Ansary, D.O.; Elansary, H.O. Influence of sowing windows and genotypes on growth, radiation interception, conversion efficiency and yield of guar. *Saudi J. Biol. Sci.* **2021**, *28*, 3453–3460. [CrossRef]
71. Chavez, J.C.; Ganjegunte, G.K.; Jeong, J.; Rajan, N.; Zapata, S.D.; Osias, R.A.; Enciso, J. Radiation use efficiency and agronomic performance of biomass sorghum under different sowing dates. *Agronomy* **2022**, *16*, 1252. [CrossRef]

72. Feng, Y.; Cui, X.; Shan, H.; Shi, Z.S.; Li, F.H.; Wang, H.W.; Zhu, M.; Zhong, X.M. Effects of solar radiation on photosynthetic physiology of barren stalk differentiation in maize. *Plant Sci.* **2021**, *312*, 111046. [CrossRef] [PubMed]
73. Sandhu, S.; Dhillon, B.S. Breeding plant type for adaptation to high plant density in tropical maize-A step towards productivity enhancement. *Plant Breed.* **2021**, *140*, 509–518. [CrossRef]
74. Fang, Y.; Xu, B.C.; Turner, N.C.; Li, F.M. Grain yield, dry matter accumulation and remobilization, and root respiration in winter wheat as affected by seeding rate and root pruning. *Eur. J. Agron.* **2010**, *33*, 257–266. [CrossRef]
75. Liu, Y.; Liao, Y.C.; Liu, W.Z. High nitrogen application rate and planting density reduce wheat grain yield by reducing filling rate of inferior grain in middle spikelets. *Crop. J.* **2021**, *9*, 412–426. [CrossRef]
76. Qiao, J.F.; Zhang, P.P.; Shao, Y.H.; Liu, J.B.; Li, C.; Zhang, M.W.; Huang, L. Effect of Different Planting Densities and Varieties on Dry Matter Production and Yield Formation of Summer Maize. *Crops* **2022**, *06*, 186–192.
77. Zhao, Y.; Huang, Y.F.; Li, S.; Chu, X.; Ye, Y.L. Improving the growth, lodging and yield of different density-resistance maize by optimising planting density and nitrogen fertilization. *Plant Soil Environ.* **2020**, *66*, 453–460. [CrossRef]
78. Wang, P.; Wang, Z.K.; Sun, X.C.; Mu, X.H.; Chen, H.; Chen, F.J.; Yuan, L.X.; Mi, G.H. Interaction effect of nitrogen form and planting density on plant growth and nutrient uptake in maize seedlings. *J. Integr. Agric.* **2019**, *18*, 1120–1129. [CrossRef]
79. Testa, G.; Reyner, A.; Blandino, M. Maize grain yield enhancement through high plant density cultivation with different inter-row and intra-row spacings. *Eur. J. Agron.* **2015**, *72*, 28–37. [CrossRef]